ARCHIVES OF ELECTRICAL ENGINEERING VOL. 71(3), pp. 549–558 (2022)

DOI 10.24425/aee.2022.141670

An approach to power system harmonic analysis based on triple-line interpolation discrete Fourier transform

LING LIU ✉, JINSONG ZHANG

[1] *Shandong Polytechnic,*
China

e-mail: ✉ *liuling95@163.com*

(Received: 14.09.2021, revised: 03.01.2022)

Abstract: The discrete Fourier transform (DFT) is a principal method for power system harmonic analysis. The fundamental frequency of the power system increases or decreases following load changes during normal operation. It is difficult to achieve synchronous sampling and integer period truncation in power harmonic analysis. The resulting spectrum leakage affects the accuracy of the measurement results. For this reason, a windowed interpolation DFT method for power system harmonic analysis to reduce errors was presented in this paper. First, the frequency domain expression of the windowed signal Fourier transform is analyzed. Then, the magnitude of the three discrete spectrum lines near the harmonic frequency point is used to determine the accurate position of the harmonic spectrum. Then, the calculation of the amplitude, frequency, and phase of harmonics is presented. The triple-line interpolation DFT can improve the accuracy of electrical harmonic analysis. Based on the algorithm, the practical rectification formulas were obtained by using the polynomial approximation method. The simulation results show that the fast attenuation of window function sidelobe is the key to reduce the error. The triple-line interpolation DFT based on Hanning, Blackman, Nuttall 3-Term windows has higher calculation accuracy, which can meet the requirements of electrical harmonic analysis.

Key words: electrical harmonic estimation, interpolation DFT, triple-line interpolation

1. Introduction

With the development of power electronic technology and devices, there are more and more nonlinear loads in the power system, which generate many harmonic components [1,2]. The grid connection of a large number of distributed power sources also brings a large number of harmonic components [3]. These have caused the problem of harmonic pollution to become more and more serious. The application of direct current transmission has made large-capacity converter and rectifier equipment increasingly widely used, and the resulting harmonic problems of the power system have a great impact on the safe and economic operation of the power system. Accurate analysis of harmonic signals is the prerequisite and key to solving the problem of harmonic pollution.

At present, the most direct and effective way to analyze the harmonic parameters of the power system is to apply the DFT algorithm [4–6]. However, due to the inherent characteristics of time-domain window and frequency-domain sampling of DFT, the signal to be measured is required to have an integer multiple relationship with the sampling interval in frequency-domain [7]. Otherwise, it is easy to cause spectrum leakage and picket fence effect. This makes errors of estimated signal parameters including frequency, amplitude, and phase, especially the phase error to be very large, which cannot meet the requirements of accurate harmonic measurement.

To improve the accuracy and precision of harmonic measurement, a hardware phase-locked loop circuit can be used to achieve synchronous sampling or a windowed interpolation DFT algorithm [8–10], wavelet analysis algorithm [11, 12], neural network algorithm [13, 14] and other algorithms. The advantage of the former method is that the signal processing is relatively simple. However, due to the slow response speed of the phase-locked loop, it is difficult to track the rapid changes of the signal frequency in time, so that real synchronous sampling cannot be realized. The latter method has a certain versatility, and the accuracy of harmonic analysis can be improved through different window functions and different algorithms. The fundamental frequency of the power system increases or decreases following load changes during normal operation. Even if the frequency tracking technology is adopted, it is hard to get strict synchronous sampling. The windowed interpolation DFT algorithm is a commonly used method. The error caused by spectrum leakage can be reduced by adopting a window function with excellent performance and performing interpolation correction on the calculation result. Jiao Lina and Du Yang [15] have studied the two-point data interpolation to improve the conventional DFT algorithm. They used the maximum and the sub-maximum to correct for the result.

This paper analyzes the problem of DFT spectrum leakage, and proposes a power harmonic analysis triple-line interpolation DFT method based on the Hanning window, the Blackman window, the Nuttall 3-Term window. This method obviously reduces the influence of spectrum leakage, greatly reduces the amount of calculation, and is easy to implement in embedded systems.

2. Spectrum leakage of DFT

2.1. Spectrum leakage

The DFT is constrained to operate on a finite set of N input values, sampled at a sample rate of f_s. The f_s/N is the interval of DFT frequency resolution. If the frequency f_o of the signal to be measured is not an integral multiple of the sampling interval f_s/N, it will cause spectrum leakage. For a single frequency signal $x(t) = A\cos(2\pi f t + \theta)$, let's sample at a rate of f_s and a discrete time signal with a sampling length of N.

$$x(n) = A\cos\left(2\pi(f_o/f_s)n + \theta\right), \qquad n \in \{0, 1, 2, \ldots, N-1\}, \tag{1}$$

where: A is the peak amplitude, θ is the initial phase angle. So, the Fourier transform of the input sequence $x(n)$ takes the form of

$$X(f) = \frac{A}{2}\left(e^{j\theta}W_R\left(2\pi(f - f_o)/f_s\right) + e^{-j\theta}W_R\left(2\pi(f - f_o)/f_s\right)\right), \tag{2}$$

where

$$W_R(f) = \frac{\sin(Nf/2)}{\sin(f/2)}\left(e^{-j\frac{N-1}{2}f}\right).$$

The expression of the discrete Fourier transform (DFT) of windowed signals is obtained by discrete sampling of (2) and ignoring the frequency peak at $-f_o$.

$$X(k) = \frac{A}{2}e^{j\theta}W_R\left(k\Delta f - f_o\right), \tag{3}$$

where: $\Delta f = f_s/N$, is the resolution in frequency domain. The magnitude frequency characteristics of $X(k)$ is shown in Fig. 1.

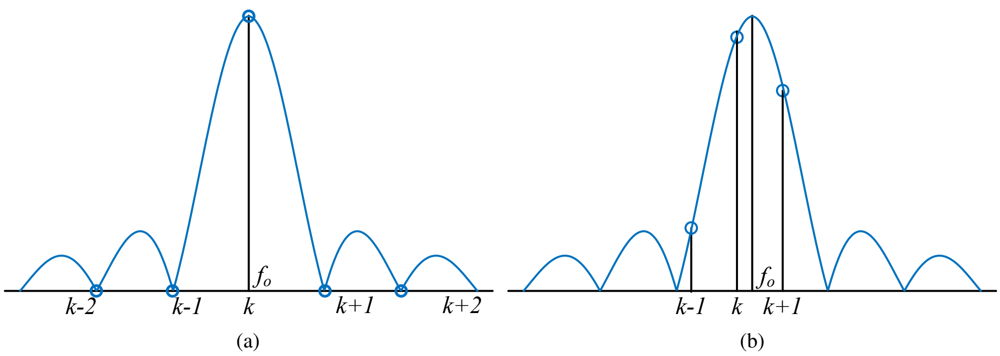

Fig. 1. Comparison of discrete spectrum between synchronous (a) and asynchronous (b) sampling

In Fig. 1(a), synchronous sampling, f_o is an integer multiple of Δf. The DFT spectrum at each discrete point is consistent with the ideal spectrum of the signal, which is an ideal pulse. In Fig. 1(b), asynchronous sampling, f_o is not an integer multiple of Δf, say $1.3\Delta f$, and the spectrum at each discrete point is inconsistent with the ideal spectrum of the signal, resulting in leakage. Therefore, the DFT calculation result must be processed to obtain the true frequency spectrum of the signal.

In fact, the power system contains rich harmonic components, and the amplitude of harmonic components is generally a few percent or less of the fundamental component. In addition, the frequency of the power system will be affected by load, which is a real-time variable, so it is difficult to measure synchronously. When asynchronous sampling is carried out, the spectrum leakage of the fundamental component will seriously affect the calculation of the harmonic component. At the same time, the harmonic components will leak into each other, resulting in the increase of harmonic analysis error.

2.2. Electrical harmonics with window function

In fact, $x(t) = A\cos(2\pi ft + \theta)$ is a signal of infinite length, intercepting a section of it is equivalent to adding a rectangular window to it. For a sine (cosine) signal, the spectrum of the original continuous signal should be at f_o frequency, which is a pulse function. Once the signal is truncated and discretized, its spectrum is shown in Fig. 1(b), and the peak is diffused. To minimize the spectral leakage, we have to reduce the sidelobe magnitude by using window functions such as the Hanning window and other cosine windows. The general expression of the combined cosine window in the time domain is

$$w(n) = \sum_{m=0}^{M-1} (-1)^m a_m \cos(2\pi nm/N), \qquad n \in \{0, 1, 2, \ldots, N-1\}, \tag{4}$$

where M is the number of items of the window function, which meets the constraints.

$$\sum_{m=0}^{M-1} a_m = 1, \qquad \sum_{m=0}^{M-1} (-1)^m a_m = 0.$$

The input sequence $x(n)$ is multiplied by the corresponding window $w(n)$ coefficients before the DFT is performed. So, the DFT of the windowed $x(n)$ input sequence $X_w(k)$ is

$$X_w(k) = \frac{A}{2} e^{j\theta} W(k\Delta f - f_o), \tag{5}$$

where $W(k)$ is the discrete Fourier transform of the window function, it takes the form of

$$W(k) = \sin(\pi k) e^{-j\frac{N-1}{N}\pi k} \sum_{m=0}^{M-1} (-1)^m \frac{a_m}{2} \cdot \left(\frac{e^{-j\frac{\pi}{N}m}}{\sin\frac{\pi}{N}(k-m)} + \frac{e^{j\frac{\pi}{N}m}}{\sin\frac{\pi}{N}(k+m)} \right). \tag{6}$$

Considering $N \gg 1$, it can be approximated as

$$W(k) = \frac{Nk\sin(\pi k)}{\pi} e^{-j\pi k} \sum_{m=0}^{M-1} (-1)^m \frac{a_m}{k^2 - m^2}\,. \tag{7}$$

3. Electrical harmonic analysis using interpolated DFT

3.1. Interpolated DFT algorithm

Suppose the digital frequency corresponding to the frequency f_o is $(k_1 + \alpha)2\pi/N$, where k_1 is a positive integer, $0 \le \alpha < 1$. In Fig. 1(a), $\alpha = 0$, $k_1/N = f_o/f_s$, there is no spectrum leakage. In Fig. 1(b), $0 < \alpha < 1$, there is a spectrum leak. In order to calculate the true frequency, the magnitudes at $k_1 - 1$, k_1 and $k_1 + 1$ shown in Fig. 1(b) can be used for correction. The magnitude at $k_1 - 1$, k_1, and $k_1 + 1$ are $|X(k_1 - 1)|$, $|X(k_1)|$, $|X(k_1 + 1)|$, where $|X(k_1)|$ is the maximum magnitude of the spectrum leak. From (2), we know that

$$\left.\begin{aligned} |X(k_1 - 1)| &= 0.5A \cdot W(-\alpha - 1) \\ |X(k_1)| &= 0.5A \cdot W(-\alpha) \\ |X(k_1 + 1)| &= 0.5A \cdot W(-\alpha + 1) \end{aligned}\right\}. \tag{8}$$

Assume

$$\beta = \frac{|X(k_1+1)|}{|X(k_1)| + |X(k_1+1)|} - \frac{|X(k_1-1)|}{|X(k_1-1)| + |X(k_1)|},$$

so, from (5),

$$\beta = \frac{|W(-\alpha+1)|}{|W(-\alpha)| + |W(-\alpha+1)} - \frac{|W(-\alpha-1)|}{|W(-\alpha-1)| + |W(-\alpha)|} = g(\alpha). \tag{9}$$

Then, we get $\alpha = g^{-1}(\beta)$. Based on this result, the actual frequency of the signal is estimated as

$$f_0 = (k_1 + \alpha)\frac{f_s}{N}. \tag{10}$$

The amplitude and phase of the signal can also be obtained by a correction function on α. In order to obtain the amplitude of the signal more accurately, use $|X(k_1-1)|$, $|X(k_1)|$, $|X(k_1+1)|$ for amplitude correction. The actual peak point amplitude is calculated by the weighted average of amplitudes of these 3 spectral lines. Considering that $|X(k_1)|$ is the maximum spectral line amplitude, give $|X(k_1)|$ a larger weight in the weighted average.

$$\begin{aligned} A &= \frac{|X(k_1-1)| + 2|X(k_1)| + |X(k_1+1)|}{0.5|W(-\alpha-1)| + |W(-\alpha)| + 0.5|W(-\alpha+1)|} \\ &= (|X(k_1-1)| + 2|X(k_1)| + |X(k_1+1)|)\, h(\alpha). \end{aligned} \tag{11}$$

The initial phase angle is estimated as

$$\theta = \text{angle}(X(k_1)) + \text{angle}(W(-\alpha)). \tag{12}$$

According to (6), we get $\text{angle}(W(-\alpha)) \approx -\pi\alpha$. Equation (12) can be approximately expressed as

$$\theta = \text{angle}(X(k_1)) - \pi\alpha. \tag{13}$$

3.2. DFT algorithm with the rectangular window

The rectangular window can be regarded as a cosine window with only one term, $M = 1$, $a_0 = 1$. The expression is

$$w_R(n) = 1, \qquad n \in \{0, 1, 2, \ldots, N-1\}. \tag{14}$$

Further, the formula in section 2.1 is simplified according to the characteristics of the rectangular window.

$$\beta = \frac{\left|\dfrac{N\cdot\sin(\pi(1-\alpha))}{\pi(1-\alpha)}\right|}{\left|\dfrac{N\cdot\sin(1-\alpha))}{\pi(1-\alpha)}\right| + \left|\dfrac{N\cdot\sin(\pi(-\alpha))}{\pi(-\alpha)}\right|} - \frac{\left|\dfrac{N\cdot\sin(\pi(-1-\alpha))}{\pi(-1-\alpha)}\right|}{\left|\dfrac{N\cdot\sin(\pi(-\alpha))}{\pi(-\alpha)}\right| + \left|\dfrac{N\cdot\sin(\pi(-1-\alpha))}{\pi(-1-\alpha)/N}\right|}. \tag{15}$$

Further simplification

$$\beta = \begin{cases} \dfrac{2\alpha^2}{-1+2\alpha}, & -0.5 < \alpha \le 0 \\ \dfrac{2\alpha^2}{1+2\alpha}, & 0 < \alpha < 0.5 \end{cases} \tag{16}$$

and

$$\alpha = \begin{cases} 0.5(\beta - \sqrt{\beta^2 - 2\beta}), & \beta \le 0 \\ 0.5(\beta + \sqrt{\beta^2 + 2\beta}), & \beta > 0 \end{cases}. \tag{17}$$

After obtaining α from β, substituting it into (10), the estimated value of the actual frequency can be obtained.

In the same way, the amplitude A can be derived as

$$h(\alpha) = \frac{\pi(\alpha - \alpha^3)}{N(1 + \alpha - \alpha^2)\sin(\pi\alpha)}. \tag{18}$$

3.3. DFT algorithm with the Hanning window

There are other window functions that reduce leakage more than the rectangle window, such as the Hanning window. The main lobe width of the Hanning window is $8\pi/N$ and is twice as wide as that of the rectangular window's. The sidelobe peak level is –32 dB, and the asymptotic decay is 18 dB/octave. The Hanning window is a 2-term cosine window, $M = 2$, $a_0 = 0.5$, $a_1 = 0.5$. The expression of the Hanning window is

$$w_{Hn}(n) = 0.5 - 0.5\cos(2\pi n/N), \quad n \in \{0, 1, 2, \ldots, N-1\}. \tag{19}$$

For the Hanning window function, it is difficult to obtain the analytical solution of α by the direct ratio method. We can use the polynomial approximation method to solve $\alpha = g^{-1}(\beta)$. The value of α is [–0.5, 0.5]. First, a set of values within this range can be substituted into (9) to obtain a set of β values. Then, we can use Matlab polynomial fitting function *Ployfit*() to calculate the coefficients of $\alpha = g^{-1}(\beta)$. So, we get

$$\alpha = 1.5\beta. \tag{20}$$

Similarly, the correction coefficient of the amplitude can be obtained by curve fitting.

$$h(\alpha) = 1.333333 + 0.526588\alpha^2 + 0.116990\alpha^4 + 0.021065\alpha^6. \tag{21}$$

3.4. DFT algorithm with the Blackman window

Along with the Hanning window, the Blackman window provides further spectral leakage reduction. The Blackman window's main lobe is almost three times as wide as the rectangular window's main lobe. The sidelobe magnitudes of the Blackman window are very small. The sidelobe peak level is –58 dB, and the asymptotic decay is 18 dB/octave. The expression of the Blackman window is

$$w_{Bm}(n) = 0.42 - 0.5\cos(2\pi n/N) + 0.08\cos(4\pi n/N), \quad n \in \{0, 1, 2, \ldots, N-1\}. \tag{22}$$

Like that of the Hanning window, the coefficients of $\alpha = g^{-1}(\beta)$ can be obtained by using the Matlab polynomial fitting function *Ployfit*().

$$\alpha = 1.991571\beta + 0.191203\beta^3 + 0.113553\beta^5 + 0.095925\beta^7 \tag{23}$$

and

$$h(\alpha) = 1.492537 + 0.490450\alpha^2 + 0.087569\alpha^4 + 0.011959\alpha^6. \tag{24}$$

3.5. DFT algorithm with the 3-term Nuttall window

Window functions are used to improve DFT spectrum analysis accuracy. When selecting a window function, we should consider not only its sidelobe attenuation characteristics, but also its progressive attenuation frequency. A small sidelobe peak and fast sidelobe attenuation rate can reduce harmonic detection error and improve detection accuracy. The Nuttall window fits these two factors. Reference [16] specifies those coefficients of the 3-term with a continuous third derivative window

$$w_{N3}(n) = (3/8) - (4/8)\cos(2\pi n/N) + (1/8)\cos(4\pi n/N), \quad n \in \{0, 1, 2, \ldots, N-1\}. \tag{25}$$

The window decays at a 30 dB/octave rate. The largest sidelobe is –46.74 dB. The coefficients of $\alpha = g^{-1}(\beta)$ can be obtained by using the Matlab polynomial fitting function *Ployfit*( ).

$$\alpha = +2.5\beta \tag{26}$$

and

$$h(\alpha) = +1.600000 + 0.454119\alpha^2 + 0.070373\alpha^4 + 0.008343\alpha^6. \tag{27}$$

4. Simulation experiment verification

4.1. Simulation

The 11th harmonic signal model used in the simulation is

$$x(n) = \sum_{i=1}^{11} \sqrt{2}A_i \cos\left(2\pi i \frac{f_o}{f_s} n + \theta_i\right), \qquad n \in \{0, 1, 2, \ldots, N-1\}, \tag{28}$$

where: f_o is the fundamental frequency, 49.80 Hz, f_s is the sampling frequency 10 000 Hz, N is the total number of sampling points, 2 048, $\sqrt{2}A_i$ is the magnitude of the fundamental wave and each harmonic, θ_i is the initial phase angle of the fundamental wave and each harmonic. The values of A_i and θ_i are shown in Table 1.

Table 1. Components of the simulated harmonic signal

Harmonics	*h*1	*h*2	*h*3	*h*4	*h*5	*h*6	*h*7	*h*8	*h*9	*h*10	*h*11
f (Hz)	49.80	99.60	149.40	199.20	249.00	298.80	348.60	398.40	448.20	498.00	547.80
A (V)	220	1.2	6.1	0.8	3.4	0.6	2.1	0.4	1.5	0.3	0.6
θ (°)	10	50	30	40	50	60	70	80	90	80	60

To minimize the spectral leakage, we have to reduce the sidelobe amplitudes by using window functions. The input DFT input signal is the discrete signal $x(n)$ multiplying by the Hanning window, the Blackman window and the Nuttall 3-Term third derivative window respectively. According to the triple-line interpolation correction formula of different windows, the frequency

Table 2. Relative errors in calculating (10^{-4}%)

Windows	Harmonics	*H*1	*H*2	*H*3	*H*4	*H*5	*H*6	*H*7	*H*8	*H*9	*H*10	*H*11
Hanning	f	0.04	174.9	0.331	–8.72	0.273	4.64	0.837	–6.65	–0.184	–1.796	0.006
	A	–0.086	3413	–1.61	117.	1.28	69.8	18.0	192	4.56	47.46	0.539
	θ	111	–57694	1613	6012	59.3	–1697	–317.	2699	114.	714	35.7
Blackman	f	0.023	164.65	0.08	–4.102	0.14	2.218	0.366	–3.048	–0.085	–0.82	0.001
	A	0.386	5415	–47.7	–102.	59.8	4.086	33.05	–18.4	3.734	–365.9	18.21
	θ	45.85	–29889	676	2578	20.6	–753	–134.	1150	49.1	312	15.5
Nuttall 3-Term	f	–0.001	–32.6	0.071	0.987	0.004	–0.293	–0.047	0.682	0.016	0.183	0.005
	A	0.014	–109.	–0.57	–9.63	–0.191	–4.36	–0.7	–13.5	–0.327	–4.476	0.043
	θ	–0.667	4293	–29.9	–273.	–1.649	78.4	11.55	–171.	–4.46	–51.4	–2.00

f_1, amplitude A_1, phase angle θ_1 are calculated separately. And the frequency f_i, amplitude A_i and initial phase θ_i of each harmonic are also calculated. The results of the simulation test are given in Table 2.

From Table 2, we can see that the calculation accuracy of frequency value is very high, and the calculation error is very small, it can reach 10^{-7}. The calculation error of phase angle is relatively large. Compared with other harmonics, the calculation error of second harmonic parameters is a little larger.

In terms of calculation speed and amount:

1. Frequency
   The frequency offset α of the interpolation algorithm with the Blackman window is the seventh polynomial of the magnitude ratio β. The amount of calculation is larger than others. In the case of the interpolation algorithm with the Hanning window or the Nuttall window, the frequency offset α is the linear relationship of the magnitude ratio β. The amount of the calculation is relatively small.
2. Amplitude
   The DFT correction algorithms with the windowed function need to calculate a sixth-degree polynomial, which increases the amount of calculation.
3. The correction of phase angle is relatively simple. So, the triple interpolation DFT correction algorithm with the Nuttall window is a good harmonic parameter calculation method.

4.2. Experiment

To verify the effectiveness of the algorithm, the function signal generator (RIGOL DG1000U) is used to send a signal as the standard signal. The frequency and phase angle of the signal are shown in Table 1, and the amplitude is 0.01 times of Table 1. The 16-bit analog-to-digital chip AD7606 is applied to the acquisition device. The input voltage range of the acquisition device is ±5 V and the sampling frequency is 10 kHz. We use the algorithm in this paper to analyze the harmonic of the collected data. The error of each parameter is shown in Table 3.

Table 3. Relative errors in experiment (10^{-4}%)

Windows	Harmonics	*H*1	*H*2	*H*3	*H*4	*H*5	*H*6	*H*7	*H*8	*H*9	*H*10	*H*11
Hanning	*f*	0.115	175.5	–0.915	–4.385	–1.49	0.004	2.27	–12.5	0.579	–8.63	0.971
	A	–1.115	3322	–1.50	–94.2	–70.6	–48.1	–15.8	411	–15.5	410	150
	θ	96.9	–57604	1784	5858	348	–1337	–601	4095	–26.5	2492	–149
Blackman	*f*	0.104	166	–1.49	2.13	–1.788	–4.155	2.207	–11.8	0.873	–7.94	0.719
	A	–1.323	936	1.21	–187.8	–77.4	–80.9	–29.3	381	–24.43	215	147.9
	θ	30.5	–29792	903	2016	348	–70.4	–495	3045	–107	2240	–99.7
Nuttall 3-Term	*f*	0.083	–32.04	–1.81	9.08	–2.09	–8.36	2.19	–10.9	1.17	–7.21	0.473
	A	–1.26	–224.6	2.04	–249.1	–81.7	–104	–37.5	358	–30.5	84.1	146
	θ	–16.4	4435	250	–1224	362	1074	–420	2213	–181	2004	–43.8

It can be seen from Table 2 and Table 3 that the accuracy of the harmonic parameter calculation decreases due to the accuracy of signal generator and data sampling error. However, the algorithm proposed in this paper can still maintain high accuracy in the calculation of frequency and amplitude.

5. Summary conclusion

The power system harmonic analysis using the constant frequency sampling DFT will cause spectrum leakage, which leads to errors in the harmonic analysis. In order to reduce the error of the harmonic analysis, a windowed interpolation DFT algorithm can be used. By adopting a window function with good performance for windowing and performing interpolation correction on the calculation result, the error caused by asynchronous sampling or non-integer period truncation of the data can be reduced. In this paper, the method of using spectrum peak three value interpolation is derived to calculate the harmonic parameters of the power system. In addition, the practical interpolation correction formula is obtained by fitting a function of Matlab. The simulation experiment results show that for harmonic analysis, the sidelobe attenuation speed of the window function is an important indicator. The window function with a fast attenuation coefficient can significantly reduce the error of harmonic analysis. The second harmonic is most affected by spectrum leakage, and the error of the calculation result is also the largest. The triple-line interpolation DFT electrical harmonic analysis method based on the Hanning window, the Blackman window and the Nuttall 3-Term third derivative window has higher calculation accuracy, a small calculation amount, and high practical value, which can meet the requirements of electrical harmonic analysis. In terms of calculation accuracy and implementation, the Nuttall window is a better choice.

References

[1] Schlabbach J., Blume D., Stephanblome T., *Voltage quality in electrical power systems*, The Institution of Engineering and Technology (2001).

[2] Yudaev I.V., Rud E.V., Yundin M.A., Ponomarenko T.Z., Isupova A.M., *Analysis of the harmonic composition of current in the zero-working wire at the input of the load node with the prevailing non-linear power consumers*, Archives of Electrical Engineering, vol. 70, no. 2, pp. 463–473 (2021), DOI: 10.24425/aee.2021.136996.

[3] Short T., *Electric Power Distribution Handbook*, Second Edition, CRC Press (2014).

[4] IEC 61000-4-30, *Testing and measurement techniques-Power quality measurement methods* (2008).

[5] IEC 61000-4-7, *Testing and measurement techniques-General guide on harmonics and interharmonics measurements and instrumentation, for power supply systems and equipment connected thereto* (2009).

[6] Jos Arrillaga, Neville R. Watson, *Power system Harmonics*, Second Edition, John Wiley & Sons, Chichester, England (2004).

[7] Lyons R.G., *Understanding Digital Signal Processing*, Second Edition, Prentice Hall PTR (2004).

[8] Pang Hao, Li Dongxia, Zu Yunxiao *et al.*, *An improved algorithm for harmonic analysis of power system using FFT Technique*, Proceedings of the CSEE, vol. 23, no. 6, pp. 50–54 (2003).

[9] Xu Y., Liu Y., Li Z., *An accurate approach for harmonic detection based on 6-term cosine window and quadruple-spectrum-line interpolation FFT*, Power System Protection and Control, vol. 44, no. 22, pp. 56–63 (2016), DOI: 10.7667/PSPC151933.

[10] Zhang C., Wang W., Qiu Y., *Detection Method of Subsynchronous Harmonic in Regions with Large Scale Wind Power Paralleled in Grid*, High Voltage Engineering, vol. 45, no. 7, pp. 2194–2202 (2019), DOI: 10.13336/j.1003-6520.hve.20181207008.

[11] Pham V.L., Wong K.P., *Wavelet-transform-based algorithm for harmonic analysis of power system waveforms*, IEE Proceedings on Generation, Transmission and Distribution, vol. 146, no. 3, pp. 249–254 (1999), DOI: 10.1049/ip-gtd:19990316.

[12] Liu Jun, Dai Benqi, Wang Zhiyue, *Power harmonic analysis based on wavelet and FFT transform*, J. Relay, vol. 35, no. 23, pp. 55–59 (2007).

[13] Cichocki A., Lobos T., *Artificial neural networks for real-time estimation of basic waveforms of voltages and currents*, IEEE Transactions on Power Systems, vol. 9, no. 2, pp. 612–618 (1994), DOI: 10.1109/59.317683.

[14] Xiang Dongyang, Wang Gongbao, Ma Weiming *et al.*, *A new method for non-integer harmonics measurement based on FFT algorithm and neutral network*, Proceedings of the CSEE, vol. 25, no. 9, pp. 35–39 (2005), DOI: 10.3321/j.issn:0258-8013.2005.09.007.

[15] Jiao L., Du Y., *An Approach for Electrical Harmonic Analysis Based on Interpolation DFT*, Archives of Electrical Engineering, vol. 71, no. 2, pp. 445–454 (2022), DOI: 10.24425/aee.2022.140721.

[16] Nuttall A.H., *Some Windows with Very Good Sidelobe Behavior*, IEEE Transactions on Acoustics Speech and Signal Processing, vol. 29, no. 1, pp. 84–91 (1981), DOI: 10.1109/TASSP.1981.1163506.